Experimental and theoretical study of angle-resolved photoemission spectra from the (1 1 1) surface of ordered CuAu I

LETTER TO THE EDITOR

Experimental and theoretical study of angle-resolved photoemission spectra from the (1 1 1) surface of ordered CuAu I

B Ginatempo†, L R Masliah‡, R G Jordan‡ and S L Qiu‡

† Dipartimento di Fisica and Unità di Ficerca INFM di Messina, Università di Messina, Salita Sperone 31, 98166 Messina, Italy
‡ Alloy Research Center, Department of Physics, Florida Atlantic University, Boca Raton, FL 33431-0991, USA

Abstract. We report an experimental and theoretical study of angle-resolved photoemission from the (1 1 1) surface of the ordered alloy CuAu I ($L1_0$) structure. The aim of the work is to test the predictions of first-principle band structure calculations by examining the fine details of the electronic structure as probed by photoemission. We compare theory with the experimental measurements not by determining an 'experimental' band structure, but rather by calculating theoretical photocurrent spectra using site potential functions determined from first-principle electronic structure calculations. We show that the one-particle theory is sufficient to explain the origin of the most important features in the experimental spectra.

In contrast to angle-integrated photoemission [1] which, apart from matrix elements effects, allows an exploration of all of the occupied electronic states in a crystal, angle-resolved photoemission spectroscopy (ARPES) probes the dispersion of the quasi-particle momentum with energy. In particular, following the greater availability and use of synchrotron radiation sources, ARPES has become the most reliable probe for investigating the validity of calculations for the (bulk) valence electronic structure of solids, once surface-related features, secondary electronic emission, electron–hole interactions, final-state effects etc have been taken into account [2, 3]. By investigating the dispersion of the peaks in photoemission spectra with photon energy or emission angle, under the assumption of a plane-wave final state for the photoelectron, 'experimental' band structure determinations have become possible [4, 5]. The approximations involved are not at all trivial, of course; quite apart from the conceptual point about the final states of photoemission being time-reversed low-energy electron diffraction (LEED) states [6, 7, 8] rather than plane waves, there are other difficulties arising from self-energy effects, the surface barrier height, and so on.

However, if band structure is the main object of the investigation by ARPES, another procedure can be adopted. Instead of determining a band structure directly from the measurements, one can use one of the main ingredients of band-structure calculations, namely the site-potential functions, to calculate, with a proper theory, photoemission spectra [9, 10, 11]. The theoretical photocurrent spectra, then, play a similar role to the experimental band structure in understanding the physics of electrons in solids. Indeed such a procedure has been successful when applied to pure metals [12]. In addition, it has been shown that one can deal also with subtle and spectacular relativistic effects [3–16] such as the spin

polarization of photoelectrons from nonmagnetic samples [17] and the intensity asymmetry of off-normal photoemission using right and left circularly polarized radiation [18].

In the case of multicomponent systems, the application of a theory of photoemission has, admittedly, a number of difficulties, mostly due to the greater complexity of alloy systems as compared with pure metals [19, 20]. Among such systems, the electronic structure in Cu–Au alloys has received a good deal of attention because of their many interesting properties, e.g. their unusual ordering properties at different stoichiometric concentrations, the physics of 'size effects' and strain fluctuations in the solid solutions phase [21], the inhomogeneity of relativistic effects (that are more important on Au sites than Cu sites [16]), the 'non-rigid' band behaviour (notwithstanding the fact that both components are noble metals), etc. However, most of the properties of Cu–Au alloys are not yet fully understood, and the purpose of this letter is to assess to what extent one can apply conventional band theoretical methods of the equi-atomic ordered alloy CuAu.

The low-temperature ordered equi-atomic phase, CuAu I, has the tetragonal $L1_0$ structure [22]. This structure can be thought of as a face-centered tetragonal lattice with a two Cu and two Au atom basis, so that there are alternate planes of Cu and Au atoms normal to the [001] direction. Along the [001] direction the lattice exhibits an experimental tetragonal distortion with a c/a ratio of 0.9251 [23]. Between about $390\,°C$ and $410\,°C$ a long period superlattice structure is stabilized, labelled CuAu II, and above $410\,°C$ a fcc solid solution phase occurs [22], albeit with some short-range ordering [24].

An ordered crystalline ingot of equi-atomic CuAu I was grown by the Bridgman method. A sample of approximately $8 \times 6 \times 1.5$ mm was removed by spark-machining with the (1 1 1) surface parallel to the largest plane. The sample was polished in the standard fashion until a mirror-smooth surface was obtained. *In-situ* cleaning in the spectrometer chamber consisted of cycles of Ne^+ ion bombardment (at 0.5 keV and at $300\,°C$) for 30 min follows by an anneal at $320\,°C$ for another 30 min; this was repeated until a clean and well-ordered (1×1) surface was obtained (as evidenced by LEED patterns). The photoemission measurements were carried out using the facilities on beam-line U4A at the NSLS, Brookhaven National Laboratory, over the photon energy range 25–100 eV. All of the spectra reported here were recorded at normal emission from the (1 1 1) surface with the light incident at an angle of $60°$ with respect with the surface normal and in the plane defined by the surface normal and the [$\bar{1}$12] direction. The polarization of the light was in the plane of the incident light and surface normal, i.e. p polarization. The overall resolution was estimated to be better than 0.2 eV over the whole photon-energy range.

In figure 1 we show the spectra obtained in the photon energy range 40–70 eV. In each spectrum the intensity has been normalized to the value of the highest peak, and no attempt has been made to subtract the secondary electron background. One can identify up to six distinct features in the spectra, labelled by the upper-case letters A to G, see figure 1. There are a number of notable changes with energy, for example; (i) features A, E, F and G at first increase with photon energy, reaching a maximum intensity around 60 eV, then decrease; (ii) feature D increases from essentially zero to a relatively large value; (iii) feature C (the reference intensity) disperses first towards the Fermi energy and then to increasing binding energy; (iv) the energy positions of D, E, F and G also change with photon energy, denoting their bulk band structure origin; (v) the energy positions of A and B, however, remain constant in energy. In fact, we identify A and B as Shockley-type surface states. (The appearance of Shockley-type surface states is a feature of the (1 1 1) surfaces of the noble metals.) The double structure arises from the fact that alternate (1 1 1) planes of the $L1_0$ structure are made up of all Cu and all Au atoms, respectively.

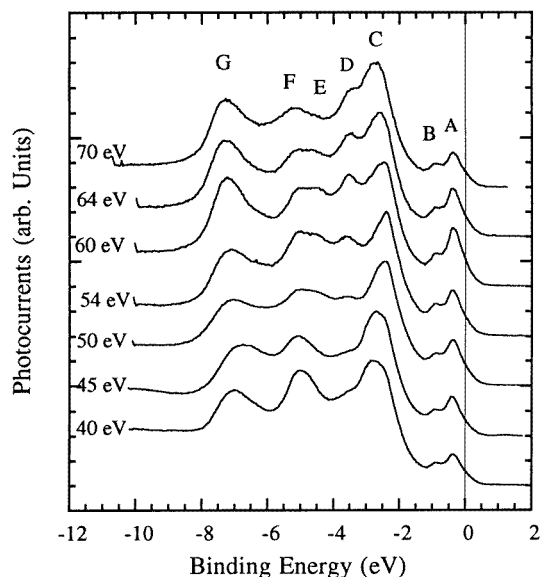In order to get a better understanding of the physics underlying the measurements we

Figure 1. The experimental photoemission spectra of CuAuI (L1$_0$ structure) taken from the (1 1 1) surface at the indicated photon energies. The geometrical set up was normal emission, with an incidence angle of 60° in the plane defined by the surface normal and the [$\bar{1}$12] direction and p polarization.

have used the relativistic theory of photoemission proposed by Ginatempo *et al* [11] to calculate the photocurrent, using previously determined Cu and Au site potential functions. According to this theory one can perform a multiple scattering calculation on a slab structure made of as many layers as are needed to take into account the photoelectron escape depth. The approach allows one to separate the full photoemission cross section into four distinct contributions, *viz*:

$$I\left(\epsilon,\ \omega,\ k_{\parallel},\ q,\ a\right) = I_{atom} + I_{intra} + I_{inter} + I_{surf} \tag{1}$$

where ϵ is the binding energy, ω is the photon frequency, $k_{\parallel}$ the photoelectron momentum parallel to the surface, q is the photon direction unit vector and a is the radiation vector potential unit vector, which defines the light polarization direction. The first term, I_{atom}, is proportional to the photocurrent one would obtain if the system was made up of an isolated atom only and the final state was the actual time-reversed LEED state. The second term, I_{intra}, the intra-layer multiple scattering correction, arises from the fact that in each layer of the slab the atoms are not isolated and so it takes into account the interference of the waves originating from all the atoms in the layer, excluding the atom at the origin. The third term, I_{inter}, the inter-layer multiple scattering correction, arises because of the interference of the forward and backward travelling waves in the slab that originate from each layer. The surface also affects the back-scattering. In fact, the surface barrier, even in the naïve step approximation, acts as a source of photoelectrons (in the case of p polarization), and, because of its non-zero reflectivity, it acts also as a source of plane waves that propagate inside the crystal and backwards to the detector. Such a wavefield contributes to I_{surf} but also significantly effects I_{inter}.

Let us assume, for a moment, that all the layers and all the atomic potentials are identical to the bulk ones. Moreover, let us model the surface by a step barrier potential centered

at $z = 0$ (with the z direction perpendicular to the surface). Under these assumptions, equation (1) will give a photocurrent spectrum as close as possible to what we might refer to as a 'bulk photoemission spectrum'. In reality, the surface profoundly affects the physics of the process because of the relaxation of the charge density and the potentials in the slab. Not only can that give rise to local electronic states at the surface but often leads to changes in the interatomic distances, composition of the layers, surface phase equilibrium and so on. Therefore the real photocurrent is bound to contain all these details. However, the bulk photocurrent (in the above sense) could still provide the main contribution to the experimental spectra, depending on the sample, the surface, the photon energy range, etc. In such cases equation (1) provides the most direct link between ARPES and the energy- and momentum-dependent quantity of interest, namely the electronic band structure.
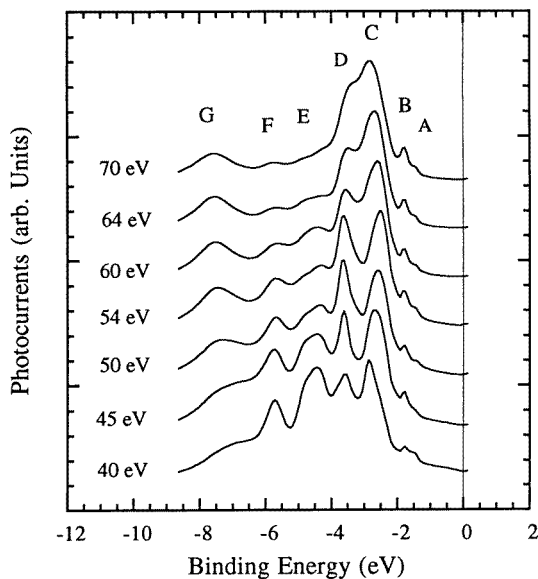

Figure 2. The theoretical 'bulk' spectra from the (1 1 1) surface of CuAu I (L1$_0$ structure) with the same geometrical configuration and the same photon energies as in figure 1.

We calculated the bulk photocurrents for the (1 1 1) surface of CuAu I using the same geometrical arrangement used for obtaining the data in figure 1; we show the results in figure 2. We used bulk Cu and Au atomic potentials produced using the SCF-LMTO-ASA method [25]; we fixed the tetragonal distortion to the experimental value but relaxed the lattice constant a to minimize the total electronic energy. The calculations are described in more detail in [26]. The SCF potentials obtained (in the ASA format) and the calculated Fermi energy were used as input to our photoemission calculations. We fixed the step barrier height (above the Fermi energy) to the weighted average tabulated values of the work functions of Cu and Au. Such a choice is of course questionable but for these preliminary calculations our purpose is, as explained above, to investigate the bulk contributions to the photocurrents, not to reproduce the experimental results! Another technical aspect of the calculation involves the inverse lifetimes of the high- and low-energy states. For the high-energy lifetimes we made a parametrization of the universal escape depth curve as a function of kinetic energy. We are uncertain how many-body effects affect the low-energy lifetime of the hole propagation in detail within the slab, but we used a quadratic form of

the type $\alpha(\epsilon - \epsilon_F)^2 + \beta$ [12].

One can see a noticeable resemblance between the calculated spectra and those in figure 1. In the calculated photocurrents we have made no attempt to reproduce the secondary electron emission and, for the sake of providing a ready comparison with the experimental measurements, each spectrum has been normalized to its respective maximum value. Limiting the discussion to the features from C to G for a moment, one can see that the energy distances of the peaks are generally well reproduced. Some small discrepancies can be traced for peaks E and F, which are rather better resolved in the theoretical spectra than in the experiment. Also peak D is somewhat too intense at the lowest photon energy compared with the measurements. However, on balance, the measurements and the calculations are in rather good agreement. (We should remark that the differences in the peaks shapes can be corrected *a posteriori* by playing around with the lifetimes, making them not only energy dependent but also state dependent.) In contrast, the agreement for peaks A and B is not as good; their relative intensities are reversed and their binding energies are too large with respect to the Fermi level. Actually, this is not surprising since, by neglecting the different charge redistribution that occurs in the surface region compared with the bulk, the model we have used for the surface is not reliable. Although we can reproduce the appearance of the surface states A and B, we will only be likely to obtain much more quantitative agreement by using a model with more realistic, surface-layer potentials.

Finally we should also note that the calculations in figure 2 are fully relativistic. Such an approach is essential in Au alloys because the relativistic interactions, namely spin–orbit, mass-velocity and Darwin terms, are much stronger at the Au site than at the Cu site. As a consequence the Au-related bands are pushed to increased binding energies, thereby increasing the split-band character of the alloy. If we use an enhanced value for the speed of light in our calculations, features G, F and E of figure 2 move towards the Fermi energy. This simple exercise shows that; (i) G, F and E are derived from Au-related states; (ii) relativity plays an important role in the photoemission from Au alloys, affecting peak positions and the hybridization; (iii) calculating theoretical bulk spectra helps one understand photoemission spectra. Thus, we conclude that the one-electron approach is sufficient to explain the origin of the most important features in the experimental photoemission spectra from the (1 1 1) surface of CuAu I.

Although the comments above could well represent the conclusions of this letter, we should add that it is possible to improve considerably the reliability of photocurrent calculations suggested by equation (1), by including surface effects more realistically. Currently it is possible to evaluate SCF slab potentials for a model that includes a surface and, in principle, they can be used in a calculation similar to that used here. Work is in progress in this direction.

References

[1] Krummacher S, Sen N, Gudat W, Johnson R, Grey F and Ghijsen J 1989 *Z. Phys. B-Condens. Matter* **75** 235
[2] Himpsel F J 1983 *Adv. Phys.* **32** 1

[3] Williams R H, Srivastava G P and McGovern I T 1980 *Rep. Prog. Phys.* **43** 1357
[4] Knapp J A, Himpsel F J and Eastman D E 1979 *Phys. Rev.* B **19** 4952
[5] Courths R, Wern H, Hau U, Cord B, Bachelier V and Hüfner S 1984 *J. Phys. F: Met. Phys.* **14** 1559
[6] Mahan G D 1970 *Phys. Rev.* B **2** 4334
[7] Schaich W L and Ashcroft N W 1971 *Phys. Rev.* B **3** 2452
[8] Caroli C, Lederer-Rozenblatt D, Roulet B and Saint-James D 1973 *Phys. Rev.* B **8** 4552
[9] Pendry J B 1976 *Surf. Sci.* **57** 679
[10] Ackerman B and Feder R 1985a *J. Phys. C: Solid State Phys.* **18** 1093
[11] Ginatempo B, Durham P J and Gyorffy B L 1989 *J. Phys.: Condens. Matter* **1** 6483
[12] Tamura E, Piepke W and Feder R 1989 *J. Phys.: Condens. Matter* **1** 6469
[13] Ginatempo B, Durham P J, Gyorffy B L and Temmermann W M 1985 *Phys. Rev. Lett.* **54** 1581
[14] Ackerman B and Feder R 1985b *Solid State Commun.* **54** 1977
[15] Ginatempo B and Gyorffy B L 1990 *J. Phys.: Condens. Matter* **2** 5233
[16] Ginatempo B, Gyorffy B L and Stocks G M 1993 *Metallic Alloys: Experimental and Theoretical Perspectives* ed J S Faulkner and R G Jordan (NATO-ASI Series E: Applied Sciences) 256 (Dordrecht: Kluwer)
[17] Eyers A A, Schafers F, Schonhense G, Heinzmann U, Oepen H P, Hunlich K, Kirschner J and Borstel G 1984 *Phys. Rev. Lett.* **52** 1559
[18] Oepen H P, Hunlich K and Kirschner J 1986 *Phys. Rev. Lett.* **56** 496
[19] Durham P J 1981 *J. Phys. F: Met. Phys.* **11** 2475
[20] Jordan R G and Durham P J 1989 *Alloy Phase Stability* ed G M Stocks and A Gonis (NATO-ASI series E: Applied Sciences) 163 (Dordrecht: Kluwer)
[21] Zunger A 1994 *Statics and Dynamics of Alloy Phase Transformations* ed P E A Turchi and A Gonis (NATO-ASI series B: Physics) 319 (Dordrecht: Kluwer)
[22] Massalski T B 1990 *Binary Alloy Phase Diagram* vol 1 (ASM International)
[23] Pearson W B 1958 *A Handbook of Lattice Spacings and Structures of Metals and Alloys* (London: Pergamon)
[24] Yamagishi K, Hashimoto S and Iwasaki H 1982 *J. Phys. Soc. Japan* **51** 605
[25] Skriver H L 1984 *The LMTO Method* (Berlin: Springer)
[26] Jordan R G, Xu Xumou, Qiu S L, Durham P J and Guo G Y 1996 *J. Phys.: Condens. Matter* **8** 1503–9